A Platform for Thermal Property Measurements and Transmission Electron Microscopy of Nanostructures

Citation: Harris, Tom, Julio Martinez, Eric Shaner, Brian S. Swartzentruber, Jianyu Huang, John Sullivan, and Gang Chen. "A Platform for Thermal Property Measurements and Transmission Electron Microscopy of Nanostructures." ASME/JSME 2011 8th Thermal Engineering Joint Conference (2011).

As Published: http://dx.doi.org/10.1115/AJTEC2011-44508

Publisher: ASME International

Persistent URL: http://hdl.handle.net/1721.1/119198

Version: Final published version: final published article, as it appeared in a journal, conference proceedings, or other formally published context

Proceedings of the ASME/JSME 2011 8th Thermal Engineering Joint Conference
AJTEC2011
March 13-17, 2011, Honolulu, Hawaii, USA

AJTEC2011-44508

A PLATFORM FOR THERMAL PROPERTY MEASUREMENTS AND TRANSMISSION ELECTRON MICROSCOPY OF NANOSTRUCTURES

Tom Harris, Julio Martinez, Eric Shaner, Brian Swartzentruber, Jianyu Huang and John Sullivan
Center for Integrated Nanotechnologies
Sandia National Laboratories
Albuquerque, New Mexico 87123

Gang Chen
Department of Mechanical Engineering
Massachusetts Institute of Technology
Cambridge, Massachusetts 02139

ABSTRACT

Measurements of the electrical and thermal transport properties of one-dimensional nanostructures (e.g., nanotubes and nanowires) typically are obtained without detailed knowledge of the specimens atomic-scale structure or defects. To address this deficiency, we have developed a microfabricated, chip-based characterization platform that enables both transmission electron microscopy (TEM) of atomic structure and defects as well as measurement of the thermal transport properties of individual nanostructures. The platform features a suspended heater line that contacts a suspended nanostructure/nanowire at its midpoint, which is placed on the platform using in-situ scanning electron microscope nanomanipulators. Because the nanostructure is suspended across a through-hole, we have used TEM to characterize the atomic and defect structure (dislocations, stacking faults, etc.) of the test sample. As a model study, we report the use of this platform to measure the thermal conductivity and defect structure of GaN nanowires. The utilization of this platform for the measurements of other nanostructures will also be discussed.

INTRODUCTION

Thermal transport in nanoscale structures has been recognized as vastly different compared to transport in bulk materials [1]. Thermal property measurements on micro- and nanoscale thin films and nanowires have revealed that the thermal conductivity of these structures can be reduced significantly compared to their bulk counterparts [2, 3], whereas measurements on carbon nanotubes have shown that the thermal conductivity of such structures can be comparable to or even surpass many forms of bulk carbon [4, 5].

A common technique for measuring the thermal properties of individual nanostructures relies on the use of microfabricated devices [6–8], because such devices facilitate a natural transition between the geometry of a nanoscale specimen and the macroscale laboratory environment. However, for the majority of electrical and thermal measurements in existence, very little is known about the measured material's microstructure, and the presence of defects in a material, surface roughness at an interface, and crystallinity can have profound effects on transport properties [1]. Only in recent years have advances been made that allow both atomic structure information to be obtained and thermal measurements to be performed on the exact same nanostructure [9–11]. Reasons for this paucity of structure-transport information are that transport measurements on single nanostructures are extremely challenging and obtaining atomic structure information on exactly the same wire measured introduces an immense level of complexity to the device fabrication.

Due to the limited number of measurements correlating a nanostructure's thermal transport properties to its atomic structure, a nanostructure-transport-property measurement platform has been developed that is compatible with a transmission electron microscope (TEM). This microfabricated device was designed to accommodate measurements of a nanowire, nanotube, nanobelt, or a slender, medium aspect-ratio portion of a thin

film or ribbon. The feature of compatibility with a TEM facilitates a powerful method for characterizing the atomic structure of a material, and complementary TEM techniques such as energy-dispersive x-ray spectroscopy and electron energy loss spectroscopy provide an invaluable means of chemical analysis on a specimen.

The work presented in this paper addresses the issue of relating a nanowire's thermal transport properties to its atomic structure by developing a microfabricated measurement platform that is compatible with a transmission electron microscope. Thermal conductivity measurements and TEM analysis on a GaN nanowire have been performed to demonstrate the capabilities of the microfabricated device. Details regarding the device's design and principle of operation are given in [12].

NANOSTRUCTURE DEVICE ASSEMBLY

Device fabrication

Microfabricated devices were produced from 4-inch, boron doped ($\rho \sim 1\,\Omega$-cm), double-side polished, [100]-oriented Si wafers. For this work, a 100 nm thick, low-stress (~ 100 MPa tensile, Si-rich), low-pressure chemical vapor deposition (LPCVD) silicon nitride (SiN_x) layer was chosen to function both as an etch mask and to form a silicon nitride membrane that could be used as a structural support for patterning a Pt heater/thermometer. A 25 nm thick layer of dry, thermal silicon dioxide (SiO_2) was grown on both surfaces of the Si wafer prior to the nitride deposition to reduce the occurrence of pinhole defects in the nitride layer. Silicon nitride membranes, of typical dimensions 10 μm by 40 μm, were formed by patterning an opening in the SiN_x/SiO_2 layer on the backside of the wafer using optical lithography and dry etching. This step was followed by a Si wet etch process consisting of tetramethylammonium hydroxide (TMAH), which resulted in a released, SiN_x membrane.

To fabricate a heater/thermometer for measuring the thermal properties of a nanostructure and to fabricate an auxiliary, integrated thermometer for measuring the device's surface temperature, combinations of electron-beam lithography (EBL), optical lithography, metal evaporation and lift-off, and dry etching were implemented. Electron-beam lithography (EBL) was utilized to define the heater line and the integrated thermometer. Optical contact lithography was used to fabricate the large-area contacts and contact pads on the perimeter of the device. The heater and integrated thermometer were formed from a Cr/Pt (3nm/100nm) layer and the large-area leads that extend outward to form contact pads for wire bonding or mechanical probing were formed from a Ti/Au (10nm/300nm) layer. Both metallization processes employed a standard liftoff procedure. To fully suspend the Pt heater/thermometer, a dry etch was performed in which only the non-metallized portion of the SiN_x membrane was exposed to the etchant. To perform this task, a soft mask was constructed from PMMA. After EBL and development, the chip then underwent a dry, fluorine-based etch, which removed the exposed SiN_x regions. The final, suspended heater/thermometer is a composite beam formed from Pt and SiN_x and is approximately 2 μm wide and 40 μm long, with 2 μm gaps on either side of the structure. Figure 1 shows optical images and SEM micrographs of a single, completed microfabricated device.

Nanowire placement and bonding

Nanowire placement across the suspended heater/thermometer near the heater's midpoint was achieved via a nanomanipulator *in situ* of a scanning electron microscope (SEM). Nanowire platinum-carbon (Pt-C) composite contacts were patterned using electron-beam induced deposition (EBID) in a dual beam SEM-FIB (focused ion beam) microscope. Encapsulating the nanowire at the contacts can greatly reduce the thermal contact resistance between the nanowire and the surface through which heat is transferred [11]. Along the nanowire, three thermal contact pads were formed; one contact between the nanowire and the suspended Pt heater line and a single contact at each of the two, adjacent boundaries. A micrograph showing the EBID Pt-C contacts on the nanowire is presented in figure 1 (c).

MEASUREMENT RESULTS AND DICUSSION

Thermal conductivity measurements

To demonstrate the capabilities of the microfabricated device, thermal conductivity measurements and transmission electron microscopy (TEM) analysis were performed on an individual GaN nanowire. A GaN nanowire with a triangularly faceted cross-section and a mild amount of taper along its growth direction [13] was placed and bonded onto the thermal measurement platform. Because of the varying cross-sectional area of the GaN nanowire, the single nanowire that was placed on the measurement platform was treated as two, distinct wires in the measurement process and in the data analysis. Through TEM analysis, the average widths of the nanowires were determined to be 215 nm and 295 nm.

Nanowire thermal conductivity measurements were performed in an evacuated cryostat at an ambient pressure of an order 10^{-6} torr. Electrical cold-wire resistance (R_o) measurements of both the suspended Pt heater line and the integrated thermometer, at modest ambient temperature excursions from 295 K ($\pm$25 K), permitted a measurement of the temperature coefficient of resistance (TCR), α, for both structures, which allows them to function as resistive thermometers.

The method for obtaining the thermal resistances of the two GaN nanowire sections and the Pt/SiN_x heater/thermometer followed the techniques described in [10, 12]. In this approach, an electrical current is used to Joule heat the suspended heater line such that the heater's average temperature is elevated above the

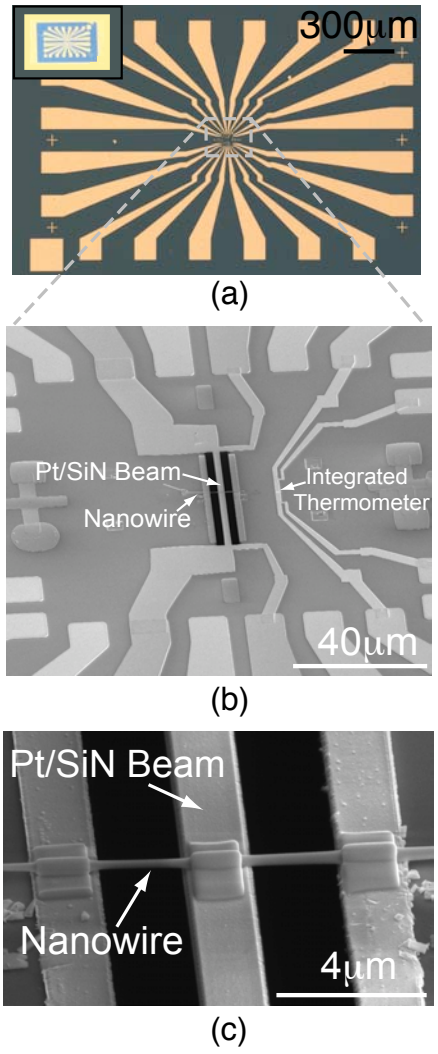

FIGURE 1. Images of the microfabricated device at various magnifications. (a) An optical image of the device's gold electrodes and contact pads. The inset (top left) shows a single microfabricated device, which is approximately 4mm by 6mm. A micrograph taken at a relatively low magnification is given in (b), which shows the nanowire placed perpendicular to the suspended heater. Also shown are the heater's current and voltage leads, and an auxiliary, integrated thermometer. (c) The nanowire after the patterning of electron beam induced deposition (EBID) Pt-C contacts.

ambient temperature. For a given input power and in the absence of a nanowire, the average temperature rise of the heater provides information regarding the thermal resistance of the suspended Pt/SiN_x composite beam, $R_{th,H}$. With a nanowire placed onto the device and making contact between the midpoint of the Pt/SiN_x heater/thermometer and the adjacent boundary, the average temperature rise of the heater provides information about the thermal resistance of the nanowire, $R_{th,NW}$. With knowledge of the heater's TCR and a measurement of the local ambient temperature, one may compute the heater's mean temperature rise above the ambient, $\Delta\overline{T}$, and the power input to the heater, $\dot{Q}$, as

$$\Delta\overline{T} = \frac{R - R_o}{\alpha R_o}, \tag{1}$$

and

$$\dot{Q} = I^2 R, \tag{2}$$

where R is the measured electrical resistance of the suspended heater/thermometer.

Thermal conductivity measurements of the two GaN nanowire sections began with the wire in the arrangement shown in figure 1 (c). To extract thermal resistance information for both sections of the nanowire, three measurements are required: one measurement with the full wire intact, a second measurement with one-half of the wire cut, and a third measurement with both halves of the wire cut. In the first measurement, both the 215 nm and the 295 nm GaN nanowire sections were intact, and a heating curve, $\Delta\overline{T}(\dot{Q})$, was generated at an ambient temperature of 295 K. In this configuration, the heating curve provides information about the total thermal resistance of the 215 nm and the 295 nm sections combined, i.e.,

$$R_{th,2NWs} = \frac{R_{th,215nm} R_{th,295nm}}{R_{th,215nm} + R_{th,295nm}}. \tag{3}$$

After the thermal measurement, TEM was performed on the 295 nm section of the wire. Once this section was examined, it was severed using an intense, local electron beam irradiation inside the TEM. After this step, the measurement-microscopy process was repeated, with the heating curves providing information about the thermal resistance of the remaining wire (i.e., $R_{th,1NW} = R_{th,215nm}$). Following this measurement, TEM imaging was performed on the 215 nm section, and the remaining wire was cut by local electron beam irradiation. With both nanowire sections disconnected from the boundary held at the ambient temperature, the measurement was repeated for a third time, which served as a calibration of $R_{th,H}$.

This cycle of measuring and cutting the nanowire after performing TEM is shown in figure 2. In this figure, transmission electron micrographs are shown of a suspended GaN nanowire that is thermally anchored at the Pt heater's midpoint and at the

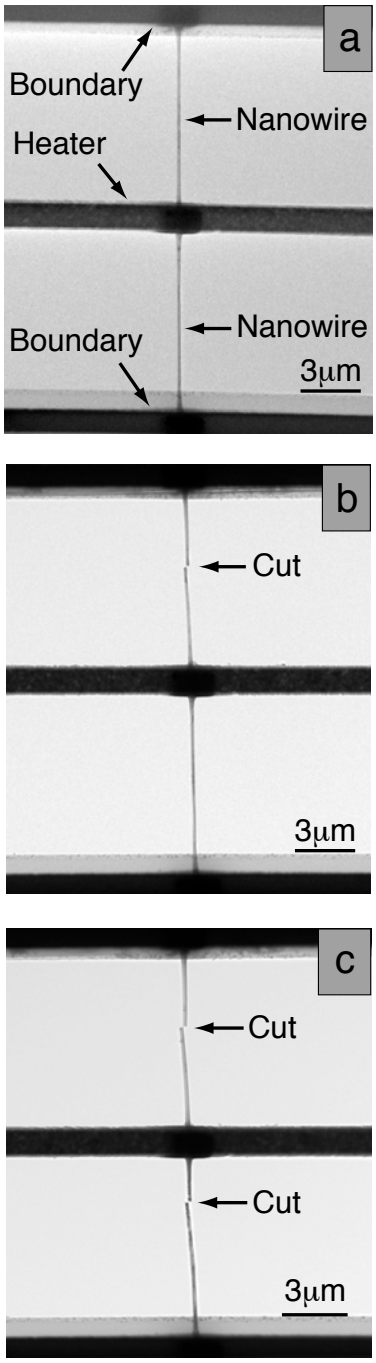

FIGURE 2. The nanowire microscopy cycle and cutting sequence. (a) Both sections of the nanowire are intact. (b) The upper nanowire has been severed using the focused electron beam in the TEM. (c) Both upper and lower sections of the nanowire have been severed.

two, adjacent boundaries. In the middle panel of figure 2 the upper nanowire has been cut, and in the bottom panel, the lower nanowire has been cut as well.

Heating-curve data taken at 295K is given in figure 3. The data presented in this plot is a combination of three, separate measurements, i.e., no nanowire cuts, one nanowire section cut, and both nanowire sections cut. From figure 3, one will note that the heater's mean temperature rise increases, for a given input power, as each nanowire section is cut. Cutting a nanowire eliminates a heat conduction path to thermal ground, and thus, the curve in which both nanowire sections have been cut is a measurement of the intrinsic thermal resistance of the heater/thermometer, $R_{\mathrm{th,H}}$.

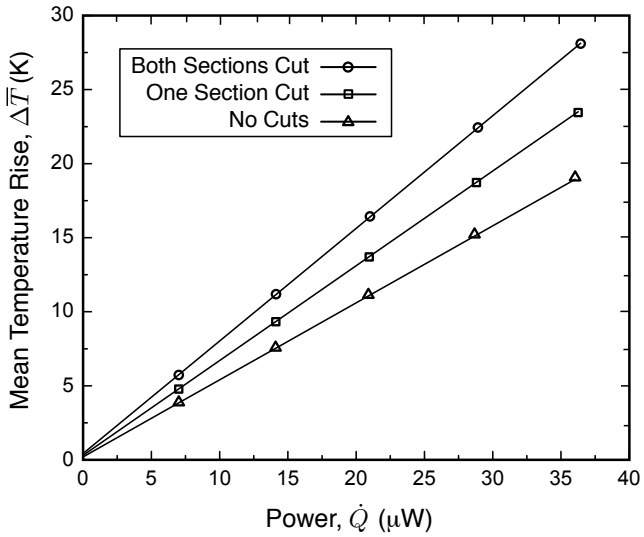

FIGURE 3. Heating curves generated at 295K. As each GaN nanowire is cut, a thermal path to ground is removed, and, for a given input power, the heater's average temperature increases.

Once the measurement-microscopy cycle had been completed, values for the thermal resistances of the suspended heater/thermometer and the 215 nm and 295 nm nanowire sections were calculated to be 6.1×10^6 K/W, 5.5×10^6 K/W, and 2.7×10^6 K/W, respectively. Based on the criteria developed in [10] for thermal impedance matching between the nanowire specimen and the heater/thermometer, the relative uncertainty in the nanowire thermal resistance was determined to be 0.4%. This uncertainty calculation is based on an observed cryostat temperature fluctuation of 10 mK, a $\Delta\overline{T} = 20$ K, and the exclusion of thermal contact resistance. By implementing a low-TCR ($0.05\,\mathrm{ppm\,K^{-1}}$), high-precision (10 ppm, 100 Ohm) current sense resistor and utilizing two SR 830 lock-in amplifiers

to perform 4-point electrical measurements on the suspended heater/thermometer, the relative uncertainty in $\dot{Q}$ was calculated to be $< 0.1\%$. An error in $\Delta\overline{T}$ due to off-center placement of the GaN nanowire with respect to the heater's midpoint may be overcome by implementing a closed-form solution for off-center placement [10]. Ignoring this off-center placement ($2\,\mu$m, here) results in an error in $\Delta\overline{T}$ of 0.6%

The existence of thermal contact resistances between the ends of the nanowire and the microfabricated device can introduce error into the measurement. To gain insight into the effects of thermal contact resistance between the nanowire and the Pt-C contact, estimates were performed using an approach similar to [6]. Measurements of the interface conductance, G_{int}, between metals, semiconductors, and insulators at room temperature have been reported with a nominal value of $G_{\text{int}} = 5 \times 10^7\,\text{W/m}^2\text{K}$ [14, 15]. Based on the geometry of the Pt-C contacts displayed in figure 1 (c), the length, l, of the contact, which is in the longitudinal direction of the nanowire, is approximately $1.5\,\mu$m. The surface area of the nanowire enclosed by the contact was calculated as $A_{\text{s}} = 3sl$, where s is the average nanowire width at the contact. From these parameters, the thermal interface resistance, $R_{\text{th,int}}$, was estimated to be $2 \times 10^4\,\text{K/W}$ for a single contact. The Pt-C contact's thermal resistance can be expressed as

$$R_{\text{th,Pt-C}} = \frac{\delta_{\text{c}}}{k_{\text{Pt-C}} A_{\text{c}}}\,, \tag{4}$$

where δ_{c} is the effective thickness of the contact and was estimated conservatively to be of an order of magnitude of the nanowire's width, $k_{\text{Pt-C}}$ is the thermal conductivity of the Pt-C composite material, and A_{c} is the area of the contact and is given approximately as $A_{\text{c}} \approx A_{\text{s}} = 3sl$. The work performed by [16] showed that EBID Pt-C structures consist of nanometer-size Pt particles embedded in an amorphous carbon matrix. Thermal conductivity measurements on amorphous carbon and amorphous silicon thin films revealed that these films possess thermal conductivities of an order 1 W/m-K [17,18]. Utilizing equation 4 and the aforementioned approximations, the thermal resistance of the Pt-C contact was estimated to be

$$R_{\text{th,Pt-C}} \approx \frac{1}{3k_{\text{c}}l} = 2 \times 10^5\,\text{K/W}. \tag{5}$$

The various Pt, SiN_x, and SiO_2 layers (and corresponding interfaces) that physically separate the Pt-C contact from the thermally anchored Si substrate each contribute thermal resistances that are of an order 10^4 K/W, which was determined based on the thin film and interface thermal property data presented in [15]. To capture the geometry of the TMAH-etched Si via, the thermal spreading resistance in the Si substrate was estimated by modeling the flow of heat into the substrate as spreading spherically from an area below the Pt-C contact into one-third of a hemispherical wedge. This thermal spreading resistance was formulated as

$$R_{\text{th,spread}} \approx \frac{3}{\pi k_{\text{Si}} d}\,, \tag{6}$$

where k_{Si} is the Si substrate's thermal conductivity and $d(= 2\,\mu\text{m})$ is the diameter of the effective contact area. Using $k_{\text{Si}} = 148\,\text{W/m-K}$ [19], the thermal spreading resistance was estimated to be $R_{th,\text{spread}} = 3 \times 10^3\,\text{K/W}$. From these estimates, the resistance to heat flow in the Pt-C contact constitutes the dominant thermal resistance. Recognizing that these contacts exist at each end of the 215 nm and 295 nm GaN nanowires, this dominant thermal contact resistance accounts for 7% and 13% of the measured thermal resistances of the 215 nm and 295 nm wires, respectively.

For a GaN nanowire with linear taper and widths at its ends of s_1 and s_2, its effective cross-sectional area, A, can be formulated as $A = \sqrt{3}s_1 s_2/4$. The thermal conductivity, k, of a GaN nanowire can be computed by relating the nanowire's thermal resistance to its thermal conductivity through

$$k = \frac{L}{R_{\text{th}} A}\,, \tag{7}$$

where L is the nanowire's length. The calculated values of thermal conductivity for both the 215 nm and 295 nm GaN nanowires are listed in table 1. The data reported in table 1 is based on each nanowire's mechanical gauge length, i.e., the length between the Pt contacts, as interpreted from an SEM micrograph. The relative uncertainties in the length and width measurements of the nanowires were due primarily to pixel resolution in the high-resolution SEM and TEM micrographs and were found to be 0.8% and 1.1%, respectively. The uncertainty in the thermal conductivity data is essentially a direct result of error introduced by the Pt-C contact thermal resistance. Also listed in table 1, for comparison, are values of the thermal conductivity for the 160 nm and 181 nm GaN nanowires measured by Guthy *et al.* [20].

TEM analysis

Transmission electron microscopy (TEM) on the GaN nanowires revealed several important attributes of the wires: the wires are single crystal, the concentration of extended defects

TABLE 1. Measured thermal conductivity, k, for the 215 nm and 295 nm GaN nanowire sections, and GaN nanowire data obtained by (Guthy *et al.*) [20]. The uncertainty in the thermal conductivity data is due to the presence of thermal contact resistance, which effectively reduces the measured thermal conductivity. The uncertainty listed in the data from Guthy is based on the scatter in their data. Also included is data for bulk GaN [21]. The corresponding temperature for all data listed is 295 K.

Specimen	k (W/m-K)
215 nm	$24.0 - 1.7$
295 nm	$25.7 - 3.3$
160 nm (Guthy)	19 ± 2
181 nm (Guthy)	18 ± 1
Bulk GaN	120

(e.g., stacking faults and dislocations) is low, a mild amount of non-uniform strain exists, and a very low concentration of Pt particle contamination resides on the wires' surfaces. The Pt contamination is a result of the electron-beam induced (EBID) Pt-C contact patterning process, and this contamination is seen as a slight mottling in the TEM images in figures 4 (a) and (b). The lower magnification image presented in figure 4 (a) reveals that the wire is under a mild amount of mechanical strain, as observed from the strain contours in the wire (i.e., the parallel lines of contrast). A high-magnification image of the wire (figure 4 (b)) exposes the Pt contamination as being small ($\leq$ 5 nm), possibly crystalline, clusters along the surface of the wire. As these Pt islands are relatively small and discontinuous, they are not expected to contribute significantly to the measured thermal conductivity of the nanowire. Figure 4 (c) is a selected-area electron diffraction pattern of the nanowire, which shows that the wire is indeed single crystalline.

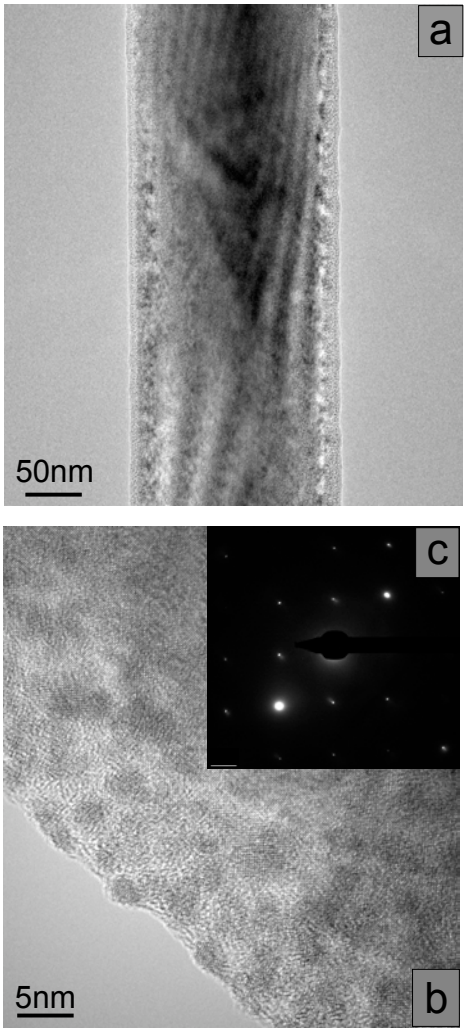

FIGURE 4. Transmission electron microscopy of the 215 nm wide GaN nanowire on the microfabricated device. (a) A TEM image of the placed GaN nanowire at a modest magnification showing a mild amount of strain in the wire. (b) A high-magnification image of one edge of the nanowire. The small crystalline clusters on the surface of the wire are the result of contamination from the EBID Pt contacts. The inset shown in (c) is a selected-area electron diffraction image and reveals the single crystal nature of the nanowire.

Discussion of results

From table 1, one may observe that all of the nanowire thermal conductivity values are lower than bulk GaN, which is approximately 120 W/m-K at 295K [21]. The thermal conductivity values for the 215 nm and 295 nm wires are quite similar in value. Interestingly, the 160 nm and 181 nm GaN nanowires exhibit similar thermal conductivity values, with the 181 nm GaN nanowire possessing a slightly lower thermal conductivity value. If the effective phonon mean free path was limited by the average width of the nanowire, one would expect a commensurate reduction in the thermal conductivity for a reduction in the width of the wire, based on classical size effects [1]. However, such a dependency appears to be weak between the various wires or perhaps lies within the measurement error. A slight reduction in thermal conductivity is apparent between the 215 nm and 295 nm wire pair and the 160 nm and 181 nm wire pair, but these sets of GaN wires were synthesized independently and measured on separate instruments. Therefore, correlating these pairs of wires directly should be done with caution. Our TEM measurements do not show a high concentration of extended defects, i.e., a de-

fect spacing shorter than the nanowire diameter. Therefore, one would not expect the phonon mean free path to be limited by scattering off of internal extended defects. Whether clusters of point defects, e.g., vacancies, could act as scattering centers in these nanowires has not yet been determined.

CONCLUSIONS

We have developed a microfabricated nanostructure thermal property measurement platform that is compatible with a transmission electron microscope. The device implements a suspended Pt/SiN_x composite beam that functions as both a heater and thermometer and utilizes resistive thermometry. Device fabrication relied on contact lithography, electron-beam lithography, and both wet and dry etching to form the Pt/SiN_x composite structure. To demonstrate the capabilities of the microfabricated device, a GaN nanowire was placed onto the device using a two-probe nanomanipulator and thermally anchored to the device with platinum-carbon (Pt-C) composite contacts. Thermal conductivity measurements of the GaN nanowire using the microfabricated device produced results very similar to existing published values for GaN nanowires. Transmission electron microscopy performed on the GaN nanowires revealed that the wires were single crystalline and possessed a minor amount of Pt contamination along the nanowires' surfaces, but no obvious defects that could potentially reduce either wires' thermal conductivity were apparent.

ACKNOWLEDGMENT

C. Thomas Harris is greatly appreciative for funding from the LDRD NINE program at Sandia National Laboratories. C. T. Harris and G. Chen are both extremely grateful for funding from NSF NIRT Award No. 0506830. The authors would like to thank George Wang of Sandia for the GaN nanowire specimen. C. T. Harris would also like to thank Chris Dames at UC Riverside for many insightful discussions on measurement and instrumentation, Patrick Hopkins at Sandia for dielectric thin film thermal characterization and useful discussions on that topic, and John Nogan at the Center for Integrated Nanotechnologies for his generosity and time in CINT's cleanroom. This work was performed, in part, at the Center for Integrated Nanotechnologies, a U.S. DOE, Office of Basic Energy Sciences user facility. Portions of this work were also supported by a Sandia National Labs LDRD project. Sandia is a multi-program laboratory operated by Sandia Corp., a wholly-owned subsidiary of Lockheed Martin Co., for the U.S. Department of Energys National Nuclear Security Administration under contract DE-AC04-94AL85000.

REFERENCES

[1] G. Chen, Nanoscale Energy Transport and Conversion: A Parallel Treatment of Electrons, Molecules, Phonons, and Photons, Oxford University Press, 2005.

[2] M. Asheghi, K. Kurabayashi, R. Kasnavi, and K. E. Goodson, "Thermal conduction in doped single-crystal silicon films", Journal of Applied Physics, (2002) 91, 5079-5088

[3] D. Li, Y. Wu, P. Kim, L. Shi, P. Yang, and A. Majumdar, "Thermal conductivity of individual silicon nanowires", Applied Physics Letters, (2003) 83, 2934-2936

[4] Yu C H, Shi L, Yao Z, Li D Y and Majumdar A 2005 Thermal conductance and thermopower of an individual single-wall carbon nanotube *Nano Letters* 5, 1842-1846

[5] Pop E, Mann D, Wang Q, Goodson K and Dai H J 2006 Thermal conductance of an individual single-wall carbon nanotube above room temperature *Nano Letters* 6, 96-100

[6] Shi L, Li D, Yu C, Jang W, Kim D, Yao Z, Kim P and Majumdar A 2003 Measuring thermal and thermoelectric properties of one-dimensional nanostructures using a microfabricated device *Journal of Heat Transfer* 125, 881-888

[7] Fujii M, Zhang X, Xie H, Ago H, Takahashi K, Ikuta T, Abe H and Shimizu T 2005 Measuring the thermal conductivity of a single carbon nanotube *Physical Review Letters* 95, 065502

[8] Fon W, Schwab K C, Worlock J M and Roukes M L 2002 Phonon scattering mechanisms in suspended nanostructures from 4 to 40K *Physical Review B* 66, 045302

[9] Mavrokefalos A, Pettes M T, Zhou F and Shi L 2007 Four-brobe measurements of the in-plane thermoelectric properties of nanofilms *Review of Scientific Instruments* 78, 034901

[10] Dames C, Chen S, Harris C T, Huang J Y, Ren Z F, Dresselhaus M S and Chen G 2007 A hot-wire probe for thermal measurements of nanowires and nanotubes inside a transmission electron microscope *Review of Scientific Instruments* 78, 104903

[11] Pettes M T and Shi L 2009 Thermal and structural characterizations of individual single-, double-, and multi-walled carbon nanotubes *Advanced Functional Materials* 19, 3918-3925

[12] Harris C T, Nanostructure Thermal Property Measurements Using a Microfabricated Suspended Hotwire *Manuscript in Preparation*

[13] Wang G T, Talin A A, Werder D J, Creighton J R, Lai E, Anderson R J and Arslan I 2006 Highly aligned, template-free growth and characterization of vertical GaN nanowires on sapphire by metal-organic chemical vapour deposition *Nanotechnology* 17, 5773-5780

[14] Cahill D G, Ford W K, Goodson K E, Mahan G D, Majumdar A, Maris H J, Merlin R and Phillpot S R 2003 Nanoscale thermal transport *Journal of Applied Physics* 93, 793-818

[15] Hopkins P E, Serrano J R, Phinney L M, Kearney S P, Grasser T W, Harris C T 2010 Criteria for cross-plane dominated thermal transport in multilayer thin film systems during modulated heating *Journal of Heat Transfer* 132, 081302

[16] Koops H W P, Kaya A, Weber M 1995 Fabrication and characterization of platinum nanocrystalline material grown by electron-beam induced deposition *Journal of Vacuum Science and Technology B* 13, 2400-2403

[17] Takahashi K, Hilmi N, Ito Y, Ikuta T, Zhang X 2009 Measurement of the thermal conductivity of nanodeposited material *International Journal of Thermophysics* 30, 1864-1874

[18] Cahill D G, Fischer H E, Klitsner T, Swartz E T, Pohl R O 1988 Thermal conductivity of thin films: measurements and understanding *Journal of Vacuum Science and Technology A* 7, 1259-1266

[19] Incropera and Dewitt 2002, *Fundamentals of Heat and Mass Transfer* (Wiley)

[20] Guthy C, Nam C Y and Fischer J E 2008 Unusually low ther- mal conductivity of gallium nitride nanowires *Journal of Applied Physics* 103, 064319

[21] Sichel E K and Pankove J I Thermal conductivity of GaN, 25-360K 1977 *Journal of Physics and Chemistry of Solids* 38, 330